Biomedicine & Pharmacotherapy 149 (2022) 112886

Contents lists available at ScienceDirect

Biomedicine & Pharmacotherapy

journal homepage: www.elsevier.com/locate/biopha

# Disclosing the antitumour potential of the marine bromoditerpene sphaerococcenol A on distinct cancer cellular models

Celso Alves [a,*], Joana Silva [a], Marta B. Afonso [b], Romina A. Guedes [b], Rita C. Guedes [b], Rebeca Alvariño [c], Susete Pinteus [a], Helena Gaspar [a,d], Márcia I. Goettert [e], Amparo Alfonso [c], Cecília M.P. Rodrigues [b], Maria C. Alpoím [f], Luis Botana [c], Rui Pedrosa [g,*]

[a] MARE—Marine and Environmental Sciences Centre, Politécnico de Leiria, 2520-630 Peniche, Portugal
[b] Research Institute for Medicines (iMed.ULisboa) Faculty of Pharmacy, Universidade de Lisboa, 1649-003 Lisbon, Portugal
[c] Department of Pharmacology, Faculty of Veterinary, University of Santiago de Compostela, 27002 Lugo, Spain
[d] BioISI - Biosystems and Integrative Sciences Institute Faculty of Science, University of Lisbon, 1749-016 Lisbon, Portugal
[e] Cell Culture Laboratory, Postgraduate Programme in Biotechnology, University of Vale do Taquari - Univates, Lajeado, RS 95914-014, Brazil
[f] Center for Neuroscience and Cell Biology (CNC), University of Coimbra, 3004-517 Coimbra, Portugal
[g] MARE—Marine and Environmental Sciences Centre, ESTM, Politécnico de Leiria, 2520-614 Peniche, Portugal

ARTICLE INFO

*Keywords:*
Algae
Marine natural products
Apoptosis
Oxidative stress
Proteasome
Cancer stem cells

ABSTRACT

Nature has revealed to be a key source of innovative anticancer drugs. This study evaluated the antitumour potential of the marine bromoditerpene sphaerococcenol A on different cancer cellular models. Dose-response analyses (0.1–100 μM; 24 h) were accomplished in eight different tumour cell lines (A549, CACO-2, HCT-15, MCF-7, NCI-H226, PC-3, SH-SY5Y, SK-MEL-28). Deeper studies were conducted on MFC-7 cells, namely, determination of hydrogen peroxide ($H_2O_2$) levels and evaluation of apoptosis biomarkers (phosphatidylserine membrane translocation, mitochondrial dysfunction, Caspase-9 activity, and DNA changes). The ability of the compound to induce genotoxicity was verified in L929 fibroblasts. Sphaerococcenol A capacity to impact colorectal-cancer stem cells (CSCs) tumourspheres (HT29, HCT116, SW620) was evaluated by determining tumourspheres viability, number, and area, as well as the proteasome inhibitory activity. Sphaerococcenol A hepatoxicity was studied in AML12 hepatocytes. The compound exhibited cytotoxicity in all malignant cell lines ($IC_{50}$ ranging from 4.5 to 16.6 μM). MCF-7 cells viability loss was accompanied by $H_2O_2$ generation, mitochondrial dysfunction, Caspase-9 activation and DNA nuclear morphology changes. Furthermore, the compound displayed the lowest $IC_{50}$ on HT29-derived tumourspheres (0.70 μM), followed by HCT116 (1.77 μM) and SW620 (2.74 μM), impacting the HT29 tumoursphere formation by reducing their number and area. Finally, the compound displayed low cytotoxicity on AML12 hepatocytes without genotoxicity. Overall, sphaerococcenol A exhibits broad cytotoxic effects on different tumour cells, increasing $H_2O_2$ production and apoptosis. It also affects colorectal CSCs-enriched tumoursphere development. These data highlight the relevance to include sphaerococcenol A in further pharmacological studies aiming cancer treatments.

## 1. Introduction

Despite the advances on cancer's biology, diagnosis and therapeutics, this disease continues to be one of the most lethal [1]. Therapy failure due to inappropriate pharmacotherapy, and tumour relapsing due to drugs resistance development, represent major clinical challenges, being reflected in patients poor prognosis [2]. Tumour's resistance to therapies can be mediated by different multifactorial events, like blockage of intracellular signaling pathways linked to cell death, metabolic adaptations of cancer stem cells (CSCs), among others [3]. Several chemotherapeutic agents have been developed to fight cancer as apoptosis inducers, proteasome inhibitors and CSCs-targeting agents, aiming to act in key biological events of tumourigenesis [4–6]. The development of therapeutic agents to eradicate cancer cells by apoptosis have been the mainstay and goal of clinical oncology in the last decades [7]. Even though several cancer cells exhibit ability to evade apoptosis, a

* Corresponding authors.
*E-mail addresses:* celso.alves@ipleiria.pt (C. Alves), rui.pedrosa@ipleiria.pt (R. Pedrosa).

https://doi.org/10.1016/j.biopha.2022.112886
Received 27 December 2021; Received in revised form 22 March 2022; Accepted 23 March 2022
Available online 1 April 2022

wide variety of stimuli and conditions, like oxidative stress, DNA damage and immune surveillance, can trigger regulated cell death [7,8]. The mechanism of action underlying several anticancer drugs (e.g. cisplatin and doxorubicin) is based on oxidative damage by boosting reactive oxygen species (ROS) production, disrupting redox homeostasis, causing severe cellular damage, leading to cancer cell death by necroptosis, ferroptosis, autophagy, and/ or apoptosis [9–11]. Furthermore, cell death mediated by those chemotherapeutic drugs seems to involve the apoptotic intrinsic pathway, since it is characterized by mitochondrial dysfunction, release of pro-apoptotic proteins, like cytochrome C, which binds to the apoptotic activating factor-1 (Apaf-1), activating "downstream" caspases, leading to chromatin condensation and DNA fragmentation [12,13].

Most of malignant cells exhibit quick cell division rates, demanding a higher protein turnover rate, to ensure protein homeostasis maintenance [14]. This cellular homeostasis is ensured by a large catalytic protease complex, named proteasome. This complex is responsible for higher percentage of protein degradation, including key regulators of biological events linked to tumourigenesis and tumour survival, like cell cycle progression, apoptosis, DNA damage and repair, cell proliferation and differentiation, among others [14,15]. The up-regulation of proteasome genes on different cancers, suggests that an efficient proteasome activity is more relevant in cancer cells than in normal cells, possibly due to their high metabolic activity, and the constant need to adapt to various stresses [16].

Tumour heterogeneity is also a key player in therapeutic resistance, since different cancer cells in tumour masses exhibit different levels of sensitivity to therapeutic drugs having a higher adaptability capacity [17,18]. Among them, CSCs, a small cellular population inside tumour masses, with self-renewal ability and multi-lineage differentiation, have been highlighted as key drivers in tumourigenesis, tumour maintenance, metastatic widespread and resistance to conventional therapeutics [19, 20]. CSCs display high plasticity, being able to remain dormant in unfavourable conditions and active when the conditions are favourable, leading to tumour relapse and metastases development [21,22]. Therefore, the discovery and development of innovative anticancer medicines targeting these biological targets improving the efficiency of current therapeutic regimens, are desirable.

Over the last decades, marine organisms have revealed to be a prolific source of unusual and distinct chemical structures with great pharmacological potential [23–25]. Bioactive marine natural products (MNPs) belonging to different chemical classes, have been reported, e.g. alcohols, alkaloids, amino acid derivatives, aromatic compounds, peptides, fatty acids, sterols, polyacetylenes, polyketides, polysaccharides, sphingolipids, lactones, and terpenes, among others [25]. Those secondary metabolites are biosynthetized as response to physical and ecological pressures being essential for organisms to survive [26–28]. Once secondary metabolites evolved over billions of years interacting with specific biological structures, their high specificity and binding affinity to biological targets make them excellent candidates for therapeutical purposes [24,29,30]. Within marine organisms, seaweeds have shown to be a relevant source of bioactive compounds, many of them with promising cytotoxic activities and ability to act on different intracellular signaling pathways linked to carcinogenesis [24].

*Sphaerococcus coronopifolius* Stackhouse 1797 is a red seaweed widely distributed in East Atlantic (Ireland, Britain and Canary Island), Mediterranean and Black Sea [31]. Its chemical profile has been studied along the last decades revealing to be a prolific source of structurally interesting diterpenes, many of them brominated [32,33]. The bromoditerpene sphaerococcenol A, firstly described by Fenical in 1979, is one of the major compounds of this specimen and is characterized to possess a sphaerane carbon skeleton [34]. This metabolite has exhibited anti-malaria [35], antimicrobial [32] and cytotoxic activities [32,36]. However, the mechanisms of action underlying its effects remain poorly known. Thus, this work aimed to evaluate the antitumour activity of sphaerococcenol A on different cancer cellular models and to study the mechanisms of action underlying its cytotoxicity. The ability to affect cancer cells with stem-like phenotype and proteasome activity was also studied. Fig. 1.

## 2. Materials and methods

### 2.1. Extraction and isolation of sphaerococcenol A

Red seaweed *Sphaerococcus coronopifolius* Stackhouse, 1797 was collected by scuba-diving in Flandres bay located in Berlenga Nature Reserve (39°24'47.9"N 9°30'28.2"W), Peniche (Portugal) with previously authorization of Instituto da Conservação da Natureza e das Florestas (ICNF). Samples were immediately transported to laboratory, cleaned, freeze-dried, and reduced to powder with a grinder. Sphaerococcenol A was isolated as previously reported [32]. Structure elucidation was determined by nuclear magnetic resonance spectroscopy and mass spectrometry techniques. Sphaerococcenol A was dissolved in dimethyl sulfoxide (DMSO) for experiments in concentrations that never exceeded 0.2%. Controls were performed with the highest concentration of DMSO as vehicle.

### 2.2. Cytotoxicity in cancer 2D - cellular models

#### 2.2.1. Cell culture maintenance

Cell lines were obtained from the American Type Culture Collection (ATCC) and from the DSMZ-German Collection of Microorganisms and Cell Cultures (DSMZ) biobanks, and cultivated according to supplier's information. L929 cells (Fibroblasts; DSMZ: ACC 2) were cultured in RPMI medium. A549 (Lung carcinoma; ATCC: CCL-185) and SH-SY5Y (Neuroblastoma; ATCC: CRL-2266) cells were cultivated in DMEM/F-12 medium (Merck, Darmstadt, Germany) supplemented with GlutaMAX™ (Gibco, Gaithersburg, MD, USA). CACO-2 (Colorectal adenocarcinoma; DSMZ: ACC 169), HCT-15 (Colorectal adenocarcinoma; DSMZ: ACC 357), MCF-7 (Breast adenocarcinoma; DSMZ: ACC 115), NCI-H226 (Lung squamous cell carcinoma; ATCC: CRL-5826), and PC-3 (Prostate adenocarcinoma; ATCC: CRL-1435) cells were cultured in RPMI medium supplemented with GlutaMAX™. SK-MEL-28 cells (Melanoma; ATCC: HTB-72) were cultivated in MEM media (Sigma, St. Louis, MO, USA). Fetal bovine serum (10%) (Biowest, Riverside, MO, USA) and 1% antibiotic/ antimycotic solution (Biowest, Nuaillé, France) were added to cell culture mediums. AML-12 (alpha mouse liver-12) hepatocytes (ATCC-CRL-2254; LGC Standards, Middlesex, UK) were grown in DMEM/F12 medium (Thermo Fisher Scientific Inc., Waltham, MA, USA) supplemented with 10% fetal bovine serum, 10 μg/mL insulin, 5.5 μg/mL transferrin, 5 ng/mL selenium (all from Gibco, Thermo Fisher Scientific Inc., MA, USA) and 40 ng/mL dexamethasone (Sigma-Aldrich, Merck, Saint Louis, MO, USA). For subculture, cells were detached with trypsin solution (Sigma-Aldrich, St. Louis, MO, USA) whenever cultures reached 80% confluence, and fresh medium was used to neutralize its

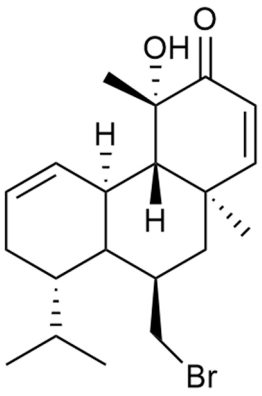


**Fig. 1.** Sphaerococcenol A chemical structure.

action. Supernatants were removed by centrifugation (290 *g*; 5 min) at room temperature. Cells were then resuspended in fresh medium (split 1–10) and seeded in 25 $cm^2$ T-Flasks. Finally, cells were cultured at 37 °C, 5% $CO_2$ and humidified atmosphere.

#### 2.2.2. Cytotoxicity assay

Cells were seeded in 96-well plates (A549: 2.5 $\times 10^5$ cells/ mL; CACO-2: 2.5 $\times 10^5$ cells/ mL; HCT-15: 2.5 $\times 10^5$ cells/ mL; MCF-7: 2.5 $\times 10^5$ cells/ mL; NCI-H226: 7.5 $\times 10^4$ cells/ mL; PC-3: 1.25 $\times 10^5$ cells/ mL; SH-SY5Y: 2.5 $\times 10^5$ cells/ mL; SK-MEL-28: 2.5 $\times 10^5$ cells/ mL; AML-12: 5.0 $\times 10^4$ cell/mL). After 24 h of seeding, cancer cell lines were exposed to sphaerococcenol A (0.1–100 μM) for 24 h and the effects assessed by the 3-(4,5-dimethylthiazol-2-yl)− 2,5-diphenyltetrazolium bromide (MTT) assay [37] with minor adjustments [38]. Cisplatin, tamoxifen, and 5-fluorouracil (all from Sigma, Shanghai, China) were used as anticancer standard controls (0.1–500 μM; 24 h). To determine compound cytotoxicity in non-cancer cells, AML-12 cells were treated with sphaerococcenol A or doxorubicin, a known hepatotoxic and cytotoxic drug, at concentrations ranging from 0.01 to 243.00 μM for 72 h. Cell viability was assessed by 3-(4,5-dimethylthiazol-2-yl)− 5-(3-carboxymethoxyphenyl)− 2-(4-sulfophenyl)− 2 H-tetrazolium (MTS) metabolism assay. The results were expressed as the half maximal inhibitory concentration ($IC_{50}$).

### 2.3. Production of hydrogen peroxide ($H_2O_2$)

Hydrogen peroxide ($H_2O_2$) levels were estimated by using Amplex™ Red hydrogen peroxide Assay kit (Molecular probes, Eugene, OR, USA) according to manufacturer's instructions. MCF-7 cells (2.5 $\times 10^5$ cells/ mL) were seeded in 96-well plates and treated with sphaerococcenol A at $IC_{50}$ and $H_2O_2$ (200.0 μM) during 1, 3, and 6 h. $H_2O_2$ generation was calculated from the slope of fluorescence curve linear phase and results expressed in percentage of control.

### 2.4. Mitochondrial membrane potential (MMP)

Mitochondrial membrane potential (MMP) was estimated by the using the JC-1 (Molecular Probes, Eugene, OR, USA) fluorescent probe [39]. MCF-7 cells (2.5 $\times 10^5$ cells/ mL) were seeded in 96-well plates and treated with sphaerococcenol A at $IC_{50}$ during 15, 30, and 60 min. FCCP (2.5 μM) (Sigma, Rehovot, Israel) plus oligomycin A (1 μg/mL) (Sigma, St. Loius, MO, USA) conjugate solution was used as positive control. Formation of JC-1 aggregates (λ excitation: 490 nm; λ emission: 590 nm), and monomers (λ excitation: 490 nm; λ emission: 530 nm) was measured during 30 min using a plate reader (Bio-Tek Synergy plate reader, Bedfordshire, UK). MMP changes were calculated from the ratio between JC-1 monomers and aggregates and presented in percentage of control.

### 2.5. Apoptosis

#### 2.5.1. Annexin V-FITC/ Propidium Iodide (PI) staining

Translocation of phosphatidylserine (Annexin V) and membrane integrity (PI) was determined using an Apoptosis Detection Kit (Immunostep, Salamanca, Spain) following the manufacturer's instructions. MCF-7 cells (1.0 $\times 10^6$ cells/ mL) were seeded in 6-well plates and exposed to sphaerococcenol A at $IC_{50}$ for 24 h. Staurosporine (1 μg/mL) (Sigma, Rehovot, Israel) was used as positive control. Cells were then incubated 1 h with probes and analysed by flow cytometry. Ten thousand events were recorded with an AMNIS imaging flow cytometer using the AMNIS INSPIRE™ software. Data were analysed using the AMNIS IDEAS™ software (Amnis Corporation v6.0, Luminex Corp, Austin, TX, USA). Results were expressed as percentage of events (viable, apoptosis, late apoptosis, necrosis).

#### 2.5.2. Caspase-9 activity

Enzyme activity was measured with the Caspase-9 Fluorimetric Assay Kit (Biovision, Milpitas, CA, USA) following the supplier' instructions. MCF-7 cells (1.0 $\times 10^6$ cells/ mL) were seeded in 6-well plates and treated with sphaerococcenol A at $IC_{50}$ for 3 and 6 h. Staurosporine (1 μg/mL) was used as positive control. Results were expressed in percentage of control (Δfluorescence (u.a)/ mg of protein/ min).

#### 2.5.3. DAPI staining

DAPI is a fluorescent stain that binds strongly to A-T-rich regions in DNA being used as a tool to visualize nuclear changes, such as fragmentation and/ or condensation, which are typical features of apoptosis [39]. MCF-7 cells (1.0 $\times 10^6$ cells/ mL) were seeded in 6-well plates and treated with sphaerococcenol A at $IC_{50}$ for 18, 24, and 36 h. Cells nuclei were analysed using a fluorescence inverted microscope (ZEISS Axio, VERT. A1, equipped with an AxioCam MRC-ZEISS camera, München, Germany) at 400x, and a representative image of each treatment was displayed.

### 2.6. Genotoxicity

DNA damage was evaluated according to the protocol established by Singh et al. [40] with minor changes [41]. L929 mouse fibroblasts (2.0 $\times 10^4$ cells/ mL) were seeded in 12-well plates and cultivated overnight. Fibroblasts were then treated with sphaerococcenol A (50 μM) and ethyl methanesulfonate (200 μg/ mL), as positive control, for 3 h. DNA damage was quantified as the amount of DNA released from the nucleolus. One hundred cells were randomly chosen, analysed, visually scored, and classified into five levels, according to tail size resulting from DNA damage. Non-overlapping was performed.

### 2.7. Proteasome activity

#### 2.7.1. Molecular docking studies

The protein three-dimensional structure was retrieved from the Protein Data Bank (www.rcsb.org) through the PDB code 4R67 (Human constitutive 20 S proteasome in complex with carfilzomib, 2.89 Å) [42]. To prepare this structure for docking calculations, all atoms (i.e. ligand, salts, waters, other chains) other than the receptor β5 and β6 subunits (chains L and M, respectively – CT-L active site) were deleted from the X-ray structure using the MOE software package (v.2019.0102) (Molecular Operating Environment; Chemical Computing Group ULC, 1010 Sherbooke St. West, Suite #910, Montreal, QC, Canada, H3A 2R7, 2021). AMBER99 forcefield was used to assign atom types and charges to each atom in the receptor. Hydrogen atoms were added, and the appropriate protonation states assigned using the Protonate-3D tool within MOE software package (pH 7.4 and T = 310 K). The structure of sphaerococcenol A was built and energy minimised using MOE. Molecular docking simulations were performed using the GOLD 5.4 software [43]. The binding site was defined to be centered in the Thr1Oγ (β5 catalytic subunit) with a 15 Å search radius. Noncovalent docking calculations were performed with the number of genetic algorithm (GA) runs set to 1000, 100% of search efficiency and selecting the ten top-ranked solutions. For the other settings the default parameters were used. First, an initial docking validation step was carried out, by performing self-docking calculations using GOLD (GoldScore, Chemscore, ChemPLP and ASP) and a exhaustiveness search of 1000 runs. All protein amino acid residues were kept rigid, whereas all single bonds of the ligands were treated as fully flexible. The docking parameters (scoring function and protein 3D structure) selected were able to successfully reproduce the experimental pose (RMSD < 2 Å between experimental and predicted pose). The docking procedure was subsequently used for the docking calculations.

To assess protein-ligand interactions, the top docking poses were submitted to detection of residue contacts using the docker implementation of PLIP [44]. Images of the compound and the PDB structures

were produced using PyMOL v.1.8.4.0.

#### 2.7.2. Proteasome activity on cell lysates

Pellets ($2.0 \times 10^6$ cells) obtained from Jurkat and K562 cells were prepared, washed with PBS (1x, pH 7.4), and lysed [45]. Cell lysates containing proteasomes were then resuspended in homogenization buffer (50 mM TRIS-HCl (pH 7.5), 100 mM KCl, 15% glycerol). Protein concentration was determined using the Pierce™ BCA protocol (Thermofisher Scientific, USA). In a 96-well plate, 25 μL lysate were seeded with 25 μL sphaerococcenol A (100 μM). In the control, 25 μL buffer were added to 25 μL of lysate. Cell lysates pre-treated with the compound were incubated over 30 min at 37 °C. Suc-Leu-Leu-Val-Tyr-AMC (97% purity, Enzo Life Sciences Inc., Farmingdale, NY USA) was used as substrate to measure thymotrypsin-like (CT-L) proteasome activity. Bortezomib (98% purity, Enovation Chemicals) was used as positive control. Fluorescence was measured (λ excitation: 360 nm; λ emission: 465 nm) using a microplate reader (Spectrafluor plus, Tecan, Salzburg, Austria), and activity was estimated in fluorescence units, being converted to percentage of proteasome inhibition.

### 2.8. Cytotoxicity in 3D spheroids enriched in cancer stem cells (CSCs)

#### 2.8.1. Effects on CSCs-enriched tumourspheres viability

Human colorectal carcinoma cell lines (HCT116, SW620, HT29) were acquired from European Collection of Authenticated Cell Cultures (ECACC) (Porton Down, UK) and cultivated under adherent conditions [46]. SW620, HT29 and HCT116 cells were cultured in DMEM, RPMI, and McCoy's 5 A mediums, respectively. For the generation of 3D spheroids, cells were grown in non-adherent conditions in serum-free DMEM/F12 medium containing 2% B27 supplement, 1% N2 supplement, 1% non-essential amino acids, 1% sodium pyruvate, 1% penicillin-streptavidin, 4 μg/mL heparin, 40 ng/mL recombinant human epidermal growth factor (all from Gibco, Thermo Fisher Scientific Inc., Waltham, MA, EUA) and 20 ng/mL recombinant human basic fibroblast growth factor (Peprotech, London, UK) [46]. After plating in 96-well plates (500 cells/ mL), cells were treated with sphaerococcenol A (0.031 – 16.0 μM) for 7 days to test its tumourspheres' formation inhibitory capacity. Following seven days of incubation, cellular viability was evaluated based on ATP metabolism (CellTiter-Glo™ luminescent cell viability assay). Luminescence signal was recorded using a GloMax®-MultiDetection. Cells were cultured at 37 °C under a humidified atmosphere of 5% $CO_2$.

#### 2.8.2. Tumoursphere formation

HT29 cells were seeded in 24-well plates ($1.0 \times 10^3$ cells/ mL) and treated with the compound at the $IC_{50}$ for 7 days. Tumoursphere images were then acquired using a brightfield microscopy with EVOSTM FL Auto2 imaging system (Invitrogen, Thermo Fisher Scientific Inc., Waltham, MA, USA). Tumoursphere number and area were determined using ImageJ analysis software.

### 2.9. Data and statistical analysis

Results are presented as mean ± standard error of the mean (SEM) and $IC_{50}$ determined by the analysis of non-linear regression by means of the equation: $y = 100/(1 + 10(X - \text{Log}IC_{50}))$. At least three independent experiments were carried out in triplicate. ANOVA with Dunnett's multiple comparison of group means analysis was performed to verify significant differences when compared with the vehicle treatment. The Tukey's test was applied for multiple comparisons. When applicable, the Student's t test was applied to verify the differences between the means of vehicle and metabolite treatment. Differences were considered significant at level of 0.05 ($p < 0.05$). The analyses were performed using IBM SPSS Statistics 24 (IBM Corporation, Armonk, NY, USA) and GraphPad v5.1 (GraphPad Software, La Jolla, CA, USA) software.

## 3. Results

### 3.1. Cytotoxicity in malignant cell lines and hepatocytes

Cytotoxicity of sphaerococcenol A was tested in malignant cell lines derived from different tissues (Table 1) and in immortalized hepatocytes (Fig. 2).

Sphaerococcenol A displayed an $IC_{50}$ range between 4.47 and 16.59 μM in cancer cell lines, being the highest potency observed in SK-MEL-28 melanoma cells and the lowest in CACO-2 colorectal adenocarcinoma cells, respectively (Table 1). Comparatively to the potency demonstrated in tumour cells, sphaerococcenol A exhibited low hepatotoxicity in AML12 cells, displaying an $IC_{50}$ value of 81.17 μM, being also significantly less cytotoxic than the anticancer drug doxorubicin ($IC_{50}$: 0.026 μM) (Fig. 2). Since sphaerococcenol A displayed a broad anti-cancer activity in different cellular lines, deeper studies were conducted in MCF-7 cells, to evaluate possible mechanisms involved in the antitumour activity.

### 3.2. Hydrogen peroxide levels

A few drugs cause severe cellular damage in cancer cells by boosting ROS generation to promote oxidative stress, leading to cellular death [47]. Thus, the $H_2O_2$ generated by MCF-7 cells after exposure to sphaerococcenol A ($IC_{50}$) for 1, 3, and 6 h was determined (Fig. 3).

The exposure of MCF-7 cells to sphaerococcenol A significantly increased the production of $H_2O_2$ after 1 and 3 h treatment, followed by a decrease at 6 h treatment. On the other hand, the treatment with $H_2O_2$ followed a different pattern with $H_2O_2$ levels raising after 6 h, comparing with vehicle situation (Fig. 3).

### 3.3. Depolarization of mitochondrial membrane potential (MMP)

Mitochondria plays a key role in several events linked to programmed cell death. Amongst them, the inner mitochondrial membrane permeability leads to the activation of different signals triggering downstream events including MMP depolarization [48]. The effects of sphaerococcenol A ($IC_{50}$) treatment on MCF-7 cells mitochondrial membrane potential was evaluated over 15, 30, and 60 min (Fig. 4).

The exposition of MCF-7 cells to sphaerococcenol A for 15, 30 and 60 min promoted mitochondrial depolarization being the highest effect observed after 15 min of incubation when compared with vehicle situation. This bromoditerpene exhibited similar profile to the conjugate solution used as positive control (Fig. 4).

### 3.4. Apoptosis

During regulated cell death distinct biological features are observed, including translocation of phosphatidylserine membrane, caspase activation, chromatin condensation, and DNA fragmentation [8]. The occurrence of those events on MCF-7 cells treated with sphaerococcenol A ($IC_{50}$) was assessed (Fig. 5).

Sphaerococcenol A decreased MFC-7 cells viability (24 h), increasing the percentage of late-stage apoptotic cells (Fig. 5A). Additionally, the compound stimulated the Caspase-9 activity after 3 and 6 h treatment (Fig. 5B) and induced DNA condensation after 18, 24 and 36 h treatment, followed by a DNA fragmentation pattern (Fig. 5C).

### 3.5. Induction of DNA damage on L929 fibroblasts

The evaluation of genotoxic effects of a new potential therapeutic agent is an essential step to determine its safety [49]. The effects of sphaerococcenol A on L929 fibroblast DNA integrity were evaluated after 3 h treatment (Fig. 6).

L929 fibroblasts DNA damage was classified in five levels, according to DNA morphological alterations. Level 0 – intact, no tail; Level 1 –

**Table 1**
$IC_{50}$ (μM) determination for sphaerococcenol A (0.1–100 μM; 24 h) in cancer cell lines.

| | | $IC_{50}$ (μM)[a] | | | |
|---|---|---|---|---|---|
| Tissue | Cells | Sphaerococcenol A | Cisplatin | Tamoxifen | 5-Fluorouracil |
| Breast | MCF-7 | 9.40 (5.24–16.87) | – | 27.19 (22.62–32.68) | – |
| Colorectal | CACO-2 | 16.59 (10.06–27.34) | – | – | 382.7 (247.2–592.3) |
| | HCT-15 | 7.11 (4.67–10.84) | | | 155.5 (103.1–234.5) |
| Lung | A549 | 11.29 (9.86–12.92) | 271.1 (155.2–473.6) | – | – |
| | NCl-H226 | 10.45 (8.60–12.69) | 172.9 (117.4–254.5) | | |
| Melanoma | SK-MEL-28 | 4.47 (2.17–9.19) | 51.52 (43.82–60.56) | – | – |
| Prostate | PC-3 | 9.74 (8.50–11.14) | 267.2 (176.8–403.9) | – | – |
| Neuroblastoma | SH-SY5Y | 4.63 (1.08–19.77) | 13.92 (10.91–17.76) | – | – |

[a] The values in parentheses represent the confidence intervals for 95%.

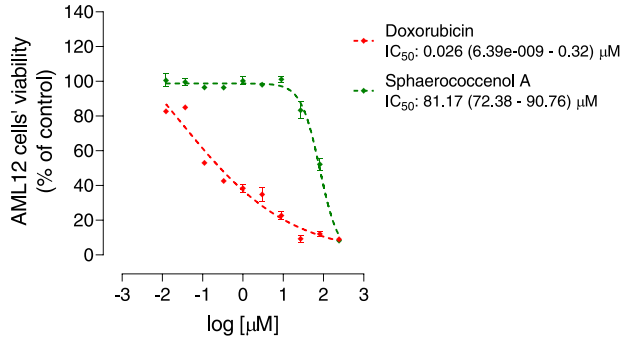


**Fig. 2.** Dose-response curves of sphaerococcenol A and doxorubicin (0.01 – 243.00 μM; 72 h) on AML12 cells.

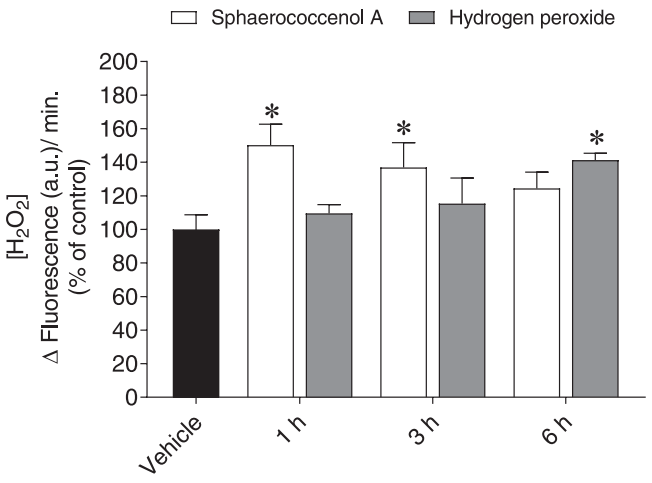


**Fig. 3.** Hydrogen peroxide ($H_2O_2$) levels produced by MCF-7 cells exposed to sphaerococcenol A (9.40 μM) for 1, 3, and 6 h. Hydrogen peroxide (200 μM) was used as positive control. Symbols represent significant differences (ANOVA, Dunnett's test, $p < 0.05$) when compared to vehicle.

short tail, smaller than the diameter of the head (nucleus); Level 2 – medium tail, 1–2 times the diameter of the head (nucleus); Level 3 – long tail, more than twice the diameter of the head (nucleus); Level 4 – very hide tail, comets without head, maximum DNA damage (Fig. 6A). Sphaerococcenol A treatment caused a slight decrease on the number of fibroblasts without DNA damage (level 0). However, when comparing

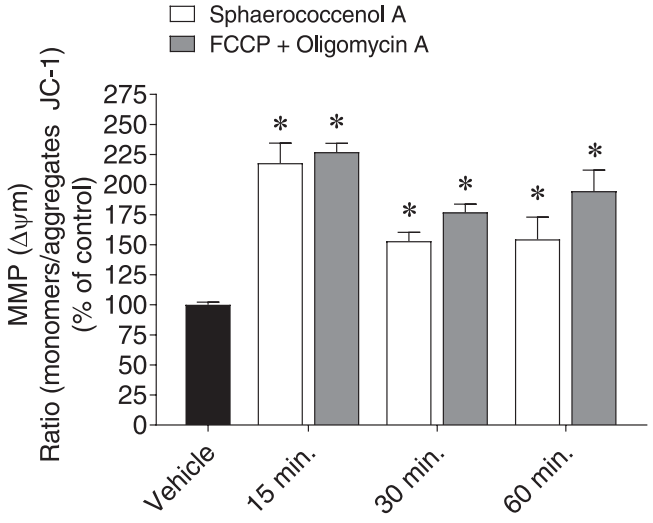


**Fig. 4.** Mitochondrial membrane potential (MMP) of MCF-7 cells exposed to sphaerococcenol A (9.4 μM) over 15, 30, and 60 min. A conjugate solution of FCCP (2.5 μM) plus oligomycin A (1 μg/mL) was used as positive control. Symbols represent significant differences (ANOVA, Dunnett's test, $p < 0.05$) when compared to vehicle.

with the vehicle situation, no significant differences were observed at 1, 2, 3, and 4 levels. On the other hand, the compound displayed significant differences at all levels when compared with the positive control (EMS) for DNA damage induction (Fig. 6B).

### 3.6. Proteasome inhibition: molecular docking predictions

Modulation of 20 S proteasome activity is a very active area of research in cancer biology. Indeed, it has been shown that proteasome inhibitors potently induce apoptosis in several types of cancer cells, while displaying a low cytotoxicity in normal cells [50]. To assess the ability of sphaerococcenol A to inhibit 20 S proteasome activity a molecular docking study was performed. The co-complex structure of human 20 S proteasome with carfilzomib (PDB code: 4R67) was used to dock sphaerococcenol A at the proteasome binding site (β5 catalytic subunit). The best docking pose of sphaerococcenol A is shown in Fig. 7.

The interaction profile of sphaerococcenol A in proteasome β5 binding site shows that although this compound is reasonably well positioned at the binding site interacting with ALA20, TYR25, TYR107, ILE109, SER129, and LYS136, it does not establish interactions with

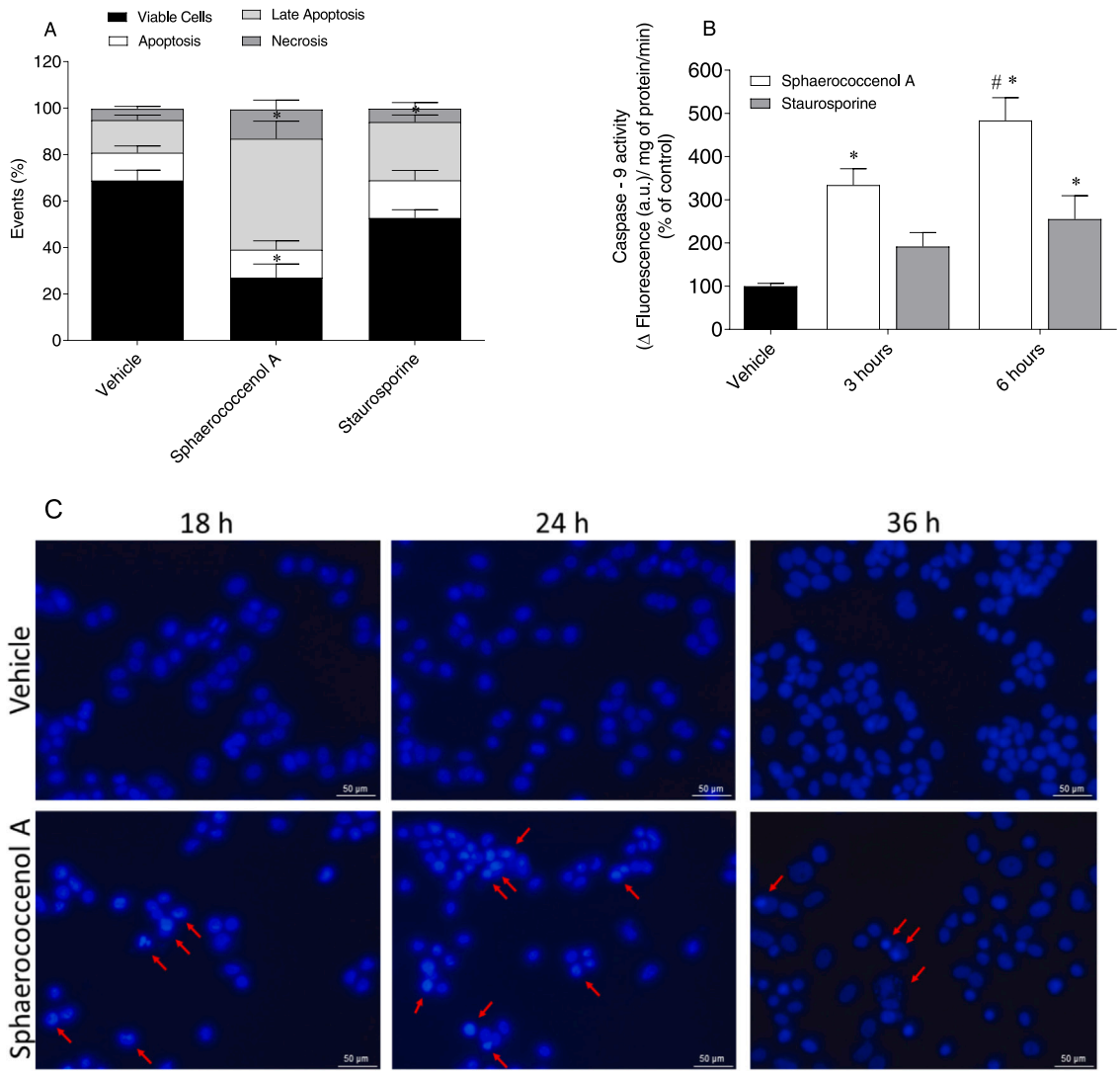


**Fig. 5.** Impact of sphaerococcenol A (9.4 µM) treatment on MCF-7 cells biological targets related with apoptosis: A) externalization of phosphatidylserine; B) Caspase-9 activity; C) DNA morphological changes. Symbols represent significant differences (Student's t test (5 A); ANOVA, Tukey's test (5B), $p < 0.05$) when compared to vehicle. Images are representative of each treatment condition.

THR1, THR2, ARG19, THR21, LYS33, MET45, ALA49, and TYR169 amino acids, that are key for recognition and proteasome inhibition. The low activity of the metabolite has been confirmed with chymotrypsin-like (CT-L) proteasomes attained from Jurkat and K562 cells lysates, inhibiting only 8% and 16%, respectively.

### 3.7. Effects on 3D colorectal spheroids enriched in CSCs

Colorectal cancer is one of the most compelling examples of a hierarchically organized solid cancer in which CSCs play a pivotal role in the metastasis and relapse [51]. Sphaerococcenol A cytotoxicity was evaluated in colorectal CSCs-enriched tumourspheres, previously established from original 2D adherent cell cultures of HT29, SW620 and HCT116 colorectal malignant cells (Fig. 8).

Sphaerococcenol A reduced HT29, SW620, and HCT116-derived tumoursphere viability in a concentration-dependent manner. The compound was more effective on HT29-enriched tumoursphere exhibiting the highest potency with a value of 0.70 µM, followed by HCT116 (1.77 µM) and SW620 (2.74 µM) derived tumourspheres (Fig. 8A). Regarding HT29 tumourspheres, sphaerococcenol A affected tumourspheres' formation, reducing significantly their number and area (Fig. 8B-D).

## 4. Discussion

Nature continues to play a key role in human health by inspiring the synthesis of innovative chemical entities with multitarget therapeutic properties and distinct mechanisms of action, contributing to the development of new medicines [52–54]. Despite this success, and the scientific community efforts, the potential of many natural anticancer agents remains poorly explored [55]. Sphaerococcenol A has been identified about four decades ago, however few studies have been carried out to assess its cytotoxic potential [32,36,56]. The data here presented suggest that the compound is not selective for a specific tumour cell line exhibiting an $IC_{50}$ range between 4.5 and 16.6 µM, which is in agreement with previous studies conducted with U373, A549, NSCLC, SK-MEL-28, PC-3, and LoVo cells (2.8–5.2 µM) [36]. Due to cancer diseases complexity, compounds acting on two or multiple cancer targets have been considered more efficient in overcoming malignant cells resistance mechanisms [57]. Thus, sphaerococcenol A capability to act on distinct biological therapeutic targets linked with oxidative stress, apoptosis and, proteasome activity in cancer cells and its influence in CSCs-enriched tumourspheres was studied. Only a grossly approach using computer-assisted phase-contrast microscopy was performed in U373 glioblastoma cells and showed a marked decrease in mitosis entry

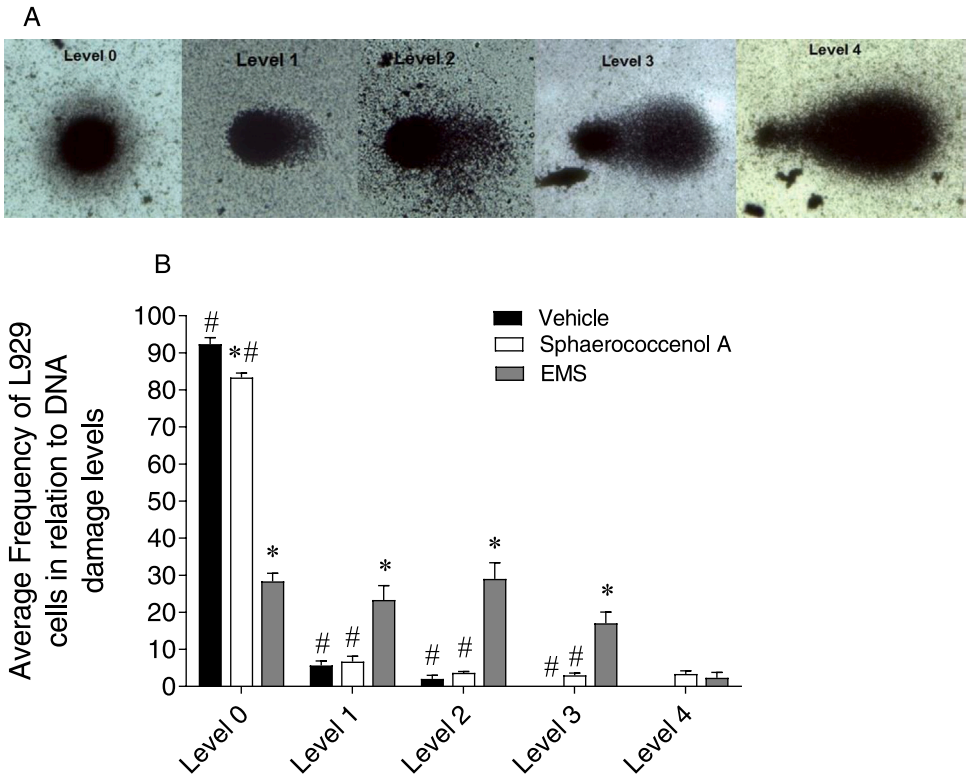


**Fig. 6.** Morphological alterations on L929 fibroblasts DNA: A) Damage index: Σ (comet class: 1, 2, 3, 4), 0 nucleus without DNA damage; B) Average frequency of L929 cells in relation to DNA damage following treatment with sphaerococcenol A (50 μM) and ethyl methanesulfonate (EMS) for 3 h. Symbols represent significant differences (ANOVA, Tukey's test, $p < 0.05$) when compared to * vehicle or #EMS.

suggesting a cytostatic effect [36]. In addition, our data suggest that the decrease in MCF-7 cells viability induced by the compound was accompanied by an increase of $H_2O_2$ levels, depolarization of mitochondrial membrane potential, and occurrence of patterns linked with apoptosis, including Caspase-9 activation and DNA damage and fragmentation. Although cell proliferation and apoptosis are distinct biological processes, they are strictly interconnected by many players, such as cell-cycle regulators and apoptotic stimulators, mediating multiple functions and influencing both processes [58–60]. Certain antineoplastic drugs induce cell cycle arrest during mitosis resulting in cytostasis, a condition poorly tolerated by any cell, and, consequently, triggering cell death by apoptosis [61]. These evidences suggest a possible relationship between the data herein obtained and the results observed by Smyrniotopoulos and co-workers [40], indicating that sphaerococcenol A may arrest the cell cycle and induce apoptosis. However, further studies need to be performed to understand the influence of this metabolite in cell cycle regulation. In MCF-7 cells, sphaerococcenol A induced $H_2O_2$ generation, a ROS known to promote cell death by apoptosis [62]. By triggering ROS levels, $H_2O_2$ can induce apoptosis through the intrinsic pathway leading to mitochondrial membrane permeability, cytochrome C release and, thereby, activating the caspase cascade [63,64]. In accordance, our previous studies have also shown that MCF-7 cells treated with $H_2O_2$ undergo depolarization of mitochondrial membrane potential and increased Caspase-9 activity [64]. Hence the data obtained suggest that the reduction of MCF-7 cells viability may be related with ROS generation and apoptosis. Other terpenoid compounds like the cembrane-type terenoid sandensolide [65], heteronemin terpenoid [66], and also spatane diterpene [67], isolated from the brown alga *Stoechospermum marginatum*, were able to increase ROS levels triggering the intrinsic apoptotic pathway. However, additional assays will be needed to attest the critical involvement of ROS in cell death induced by sphaerococcenol A, such as the study of cells' viability in the presence or absence of antioxidant molecules, such as NAC (*N*-acetyl-cysteine), which has the ability to neutralize these species. For instance, cladosporol A induces cell death by apoptosis triggered by increased ROS levels, as confirmed by a reduced effect of the compound in the presence of an antioxidant [68]. Moreover, to deeply characterize the activation of apoptosis by sphaerococenol A, further studies should be conducted targeting other biomarkers (e.g. Caspase-8, cytochrome C release, Caspase-7, Bcl-2 family proteins expression), applying different techniques such as ELISA and/or Western blot, to support the data here attained.

Other relevant therapeutic target on malignant cells is the proteasome, which seems to play a relevant role in the maintenance of malignant cells due to their high metabolic activity and requirements to adapt to distinct stresses [16]. Previous studies reported the ability of marine terpenes to act as proteosome inhibitors, inhibiting ChT-L and T-L sites, increasing the accumulation of ubiquitinated proteins [69,70]. However, although sphaerococcenol A was reasonably well positioned at the binding site, the metabolite did not establish interactions with the essential amino acids for recognition and proteasome inhibition. Moreover, the molecular docking data were reinforced by experimental assays carried out with cell lysates suggesting that the proteasome is unlikely to be the preferred target of this compound.

As previously reported, tumour heterogeneity plays a critical role in therapeutic resistance due to the presence of cancer cells with distinct features, such as CSCs. Previous studies have reported the ability of marine natural products to impact the development of these type of malignant cells, such as polysaccharides [71], carotenoids [72], and terpenes [38,73–75]. Those compounds decreased viability, number, and area of CSCs-enriched tumourspheres derived from distinct tissues, and modulated the expression levels of several genes/ proteins linked with stemness properties such as SOX2, Oct4 and Nanog. Our data obtained with sphaerococcenol A is in agreement with these observations, since it decreased the viability of different colorectal CSCs-enriched tumourspheres, particularly HT29 spheroids. Furthermore, this

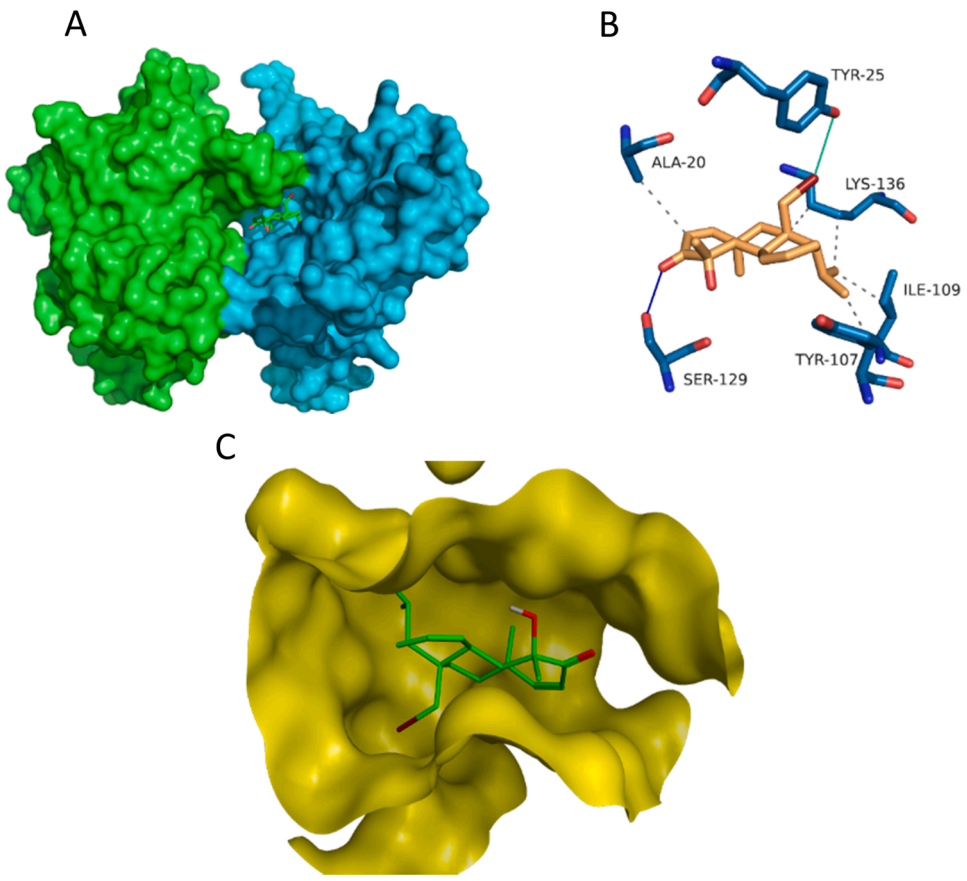


**Fig. 7.** Best docking pose of sphaerococcenol A in β5 proteosome catalytic site: A) sphaerococcenol A at the interface of proteasome β5 (cyan) and β6 (green) subunits; B) Interaction of sphaerococcenol A with β5 binding site amino acids; C) sphaerococcenol A pose in the β5 binding pocket.

metabolite also significantly impacted the number and area of those cells at sub-cytotoxic concentrations. The attained results will be relevant to further understand sphaerococcenol A effects on different intracellular signaling pathways as well as in the expression of markers related with CSCs development. Previous studies have reported the ability of compounds to increase ROS levels leading to CSCs death by ferroptosis [76,77]. Since sphaerococcenol A was able to stimulate $H_2O_2$ production, inducing a marked cytotoxic effect in 3D spheroids, the cellular death mechanism may be related with ferroptosis. The inability of sphaerococcenol A to induce DNA damage on L929 cells and cytotoxicity towards AML2 cells suggest that the compound is relatively safe for non-malignant cell, even though additional studies are required. However, despite the promising effects displayed by sphaerococcenol A on *in vitro* cellular models, it is critical to evaluate its effects in more complex models, such as human tumours xenograft models, to validate its pharmacological potential for cancer treatments. To the best of our knowledge, this is the first study characterizing the mechanisms involved in the cytotoxic activity of sphaerococcenol A. The data here attained suggest that its cytotoxicity may be related with increased $H_2O_2$ levels and induction of cancer cell death by apoptosis. Furthermore, this metabolite also influenced the number, area, and viability of colorectal CSCs-enriched tumourspheres. These results open new research hypothesis to fully explore the potential of this metabolite for cancer treatment.

## Funding

This work was supported by the Portuguese Foundation for Science and Technology (FCT) through the strategic project granted to MARE—Marine and Environmental Sciences Centre (UIDP/04292/2020, UIDB/04292/2020), BioISI—BioSystems and Integrative Sciences Institute (UIDP/Multi/04046/2020, UIDB/04046/2020), and iMed. University of Lisbon (UIDB/04138/2020, UIDP/04138/2020). This study was also supported by FCT through the POINT4PAC (SAICTPAC/0019/ 2015-LISBOA- 01–0145-FEDER-016405), PDTC/QEQ-MED/7042/2014 and CROSS-ATLANTIC (PTDC/BIA-OUT/29250/2017, co-financed by COMPETE (PO-CI-01–0145-FEDER-029250)) projects. Spanish part was funded by Conselleria de Cultura, Educacion e Ordenación Universitaria, Xunta de Galicia, GRC (ED431C 2021/01). This work was also supported by FCT and CAPES cooperation agreement through project MArTics (FCT/DRI/CAPES 2019.00277. CBM). Rebeca Alvariño is supported by a fellowship from Xunta de Galicia (ED481B-2021–038), Spain.

## CRediT authorship contribution statement

**CA:** Investigation, Methodology, Formal analysis, Writing – original draft, Visualization. **JS, MBA, RAG, RA, SP, HG, MG:** Investigation, Methodology, Formal analysis, Writing – original draft, Visualization, Writing – review & editing. **RCG, AA, CMPR, MCA, LB:** Conceptualization, Validation, Resources, Writing – review & editing, Funding acquisition, Supervision. **RP:** Conceptualization, Validation, Resources, Writing – review & editing, Funding acquisition, Supervision, Project administration.

## Conflict of interest statement

The authors declare that they have no known competing financial interests or personal relationships that could have appeared to influence the work reported in this paper.

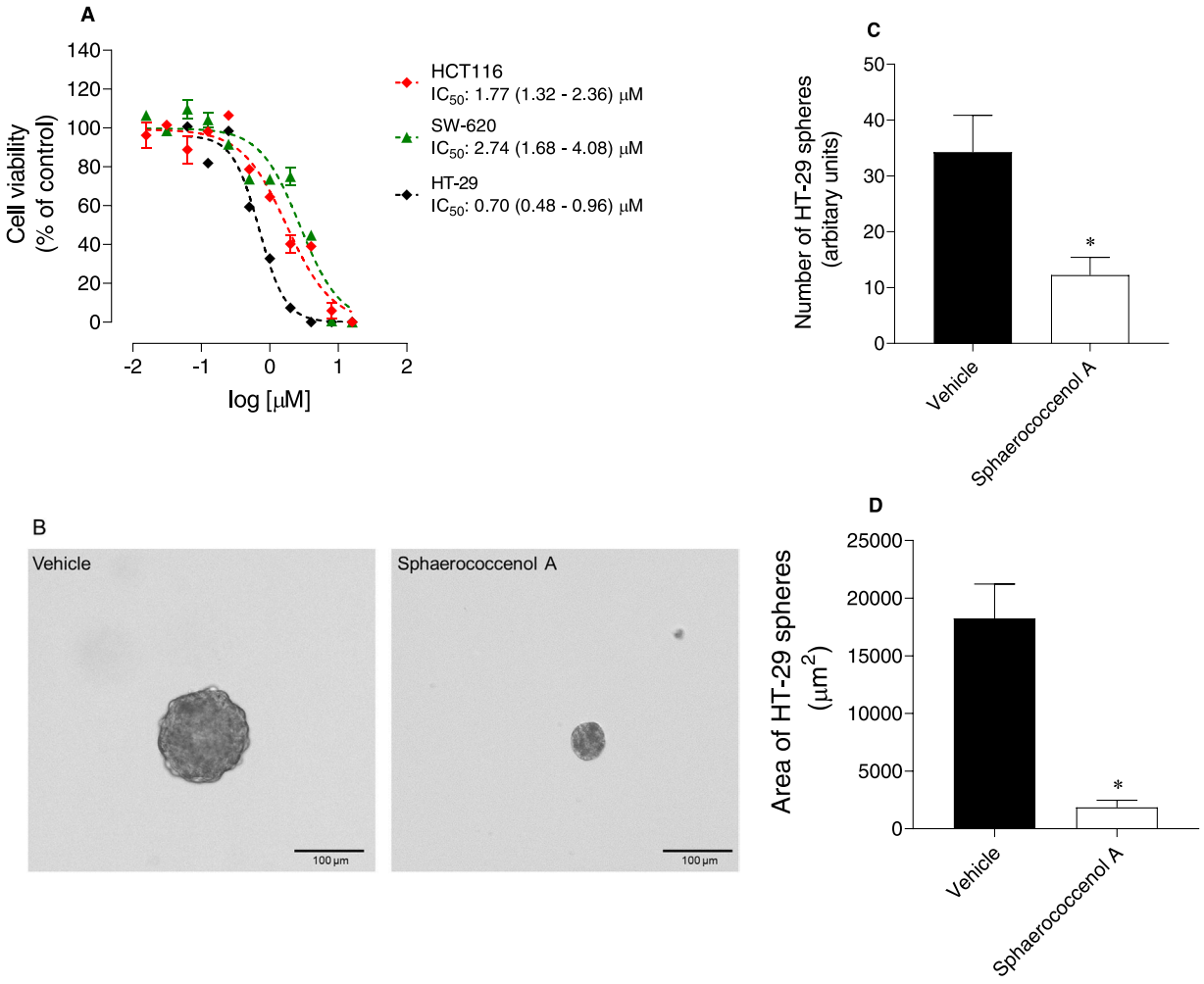


**Fig. 8.** Sphaerococcenol A effects on colorectal CSCs-enriched tumourspheres over 7 days treatment: A) Dose-response (0.031 – 15.0 μM) analysis in HT29, SW620 and HCT116 CSCs-enriched tumourspheres; B) Representative images of HT29 tumourspheres (Scale bar: 100 μm); C) Number of HT29 tumoursphere formation following treatment with $IC_{50}$; D) HT29 tumoursphere area ($\mu m^2$) following treatment with $IC_{50}$. Symbols represent significant differences (Student's t test, $p < 0.05$) when compared to vehicle.

## Data availability

Data will be made available on request.

## References


[1] Sung, H.; Ferlay, J.; Siegel, R.L.; Laversanne, M.; Soerjomataram, I.; Jemal, A.; Bray, F. Global Cancer Statistics 2020: GLOBOCAN Estimates of Incidence and Mortality Worldwide for 36 Cancers in 185 Countries. 2021, 71, 209–249, doi: https://doi.org/10.3322/caac.21660.

[2] X. Wang, H. Zhang, X. Chen, Drug resistance and combating drug resistance in cancer, Cancer Drug Resist. 2 (2019) 141–160, https://doi.org/10.20517/cdr.2019.10.

[3] Y. Li, Z. Wang, J.A. Ajani, S. Song, Drug resistance and cancer stem cells, Cell Commun. Signal. 19 (2021) 19, https://doi.org/10.1186/s12964-020-00627-5.

[4] M. Shibata, M.O. Hoque, Targeting cancer stem cells: a strategy for effective eradication of cancer, Cancers 11 (2019) 732, https://doi.org/10.3390/cancers11050732.

[5] S. Baig, I. Seevasant, J. Mohamad, A. Mukheem, H.Z. Huri, T. Kamarul, Potential of apoptotic pathway-targeted cancer therapeutic research: Where do we stand?, -e2058, Cell Death Dis. 7 (2016), e2058, https://doi.org/10.1038/cddis.2015.275.

[6] E.E. Manasanch, R.Z. Orlowski, Proteasome inhibitors in cancer therapy, Nat. Rev. Clin. Oncol. 14 (2017) 417–433, https://doi.org/10.1038/nrclinonc.2016.206.

[7] B.A. Carneiro, W.S. El-Deiry, Targeting apoptosis in cancer therapy, Nat. Rev. Clin. Oncol. 17 (2020) 395–417, https://doi.org/10.1038/s41571-020-0341-y.

[8] R. Jan, G.-E.S. Chaudhry, Understanding apoptosis and apoptotic pathways targeted cancer therapeutics, Adv. Pharm. Bull. 9 (2019) 205–218, https://doi.org/10.15171/apb.2019.024.

[9] S.J. Kim, H.S. Kim, Y.R. Seo, Understanding of ROS-inducing strategy in anticancer therapy, Oxid. Med. Cell. Longev. 2019 (2019), 5381692, https://doi.org/10.1155/2019/5381692.

[10] J. Van Loenhout, M. Peeters, A. Bogaerts, E. Smits, C. Deben, Oxidative stress-inducing anticancer therapies: taking a closer look at their immunomodulating effects, Antioxidants 9 (2020) 1188, https://doi.org/10.3390/antiox9121188.

[11] Y. Wang, H. Qi, Y. Liu, C. Duan, X. Liu, T. Xia, D. Chen, H.-L. Piao, H.-X. Liu, The double-edged roles of ROS in cancer prevention and therapy, Theranostics 11 (2021) 4839–4857, https://doi.org/10.7150/thno.56747.

[12] B. Perillo, M. Di Donato, A. Pezone, E. Di Zazzo, P. Giovannelli, G. Galasso, G. Castoria, A. Migliaccio, ROS in cancer therapy: the bright side of the moon, Exp. Mol. Med. 52 (2020) 192–203, https://doi.org/10.1038/s12276-020-0384-2.

[13] R. Pariente, J.A. Pariente, A.B. Rodríguez, J. Espino, Melatonin sensitizes human cervical cancer HeLa cells to cisplatin-induced cytotoxicity and apoptosis: effects on oxidative stress and DNA fragmentation, J. Pineal Res. 60 (2016) 55–64, https://doi.org/10.1111/jpi.12288.

[14] X. Zhang, S. Linder, M. Bazzaro, Drug development targeting the ubiquitin–proteasome system (UPS) for the treatment of human cancers, Cancers 12 (2020) 902.

[15] C.L. Soave, T. Guerin, J. Liu, Q.P. Dou, Targeting the ubiquitin-proteasome system for cancer treatment: discovering novel inhibitors from nature and drug repurposing, Cancer Metastas-.-. Rev. 36 (2017) 717–736, https://doi.org/10.1007/s10555-017-9705-x.

[16] A.V. Morozov, V.L. Karpov, Proteasomes and several aspects of their heterogeneity relevant to cancer, Front. Oncol. (2019) 9, https://doi.org/10.3389/fonc.2019.00761.

[17] I. Dagogo-Jack, A.T. Shaw, Tumour heterogeneity and resistance to cancer therapies, Nat. Rev. Clin. Oncol. 15 (2018) 81–94, https://doi.org/10.1038/nrclinonc.2017.166.

[18] Z.-F. Lim, P.C. Ma, Emerging insights of tumor heterogeneity and drug resistance mechanisms in lung cancer targeted therapy, J. Hematol. Oncol. 12 (2019) 134, https://doi.org/10.1186/s13045-019-0818-2.

[19] A.Z. Ayob, T.S. Ramasamy, Cancer stem cells as key drivers of tumour progression, J. Biomed. Sci. 25 (2018) 20, https://doi.org/10.1186/s12929-018-0426-4.

[20] K. Dzobo, D.A. Senthebane, C. Ganz, N.E. Thomford, A. Wonkam, C. Dandara, Advances in therapeutic targeting of cancer stem cells within the tumor microenvironment: an updated review, Cells 9 (2020), https://doi.org/10.3390/cells9081896.

[21] W. Chen, J. Dong, J. Haiech, M.C. Kilhoffer, M. Zeniou, Cancer stem cell quiescence and plasticity as major challenges in cancer therapy, Stem Cells Int. 2016 (2016), 1740936, https://doi.org/10.1155/2016/1740936.

[22] Y. Zhao, Q. Dong, J. Li, K. Zhang, J. Qin, J. Zhao, Q. Sun, Z. Wang, T. Wartmann, K. W. Jauch, et al., Targeting cancer stem cells and their niche: perspectives for future therapeutic targets and strategies, Semin. Cancer Biol. 53 (2018) 139–155, https://doi.org/10.1016/j.semcancer.2018.08.002.

[23] S.A.M. Khalifa, N. Elias, M.A. Farag, L. Chen, A. Saeed, M.F. Hegazy, M. S. Moustafa, A. Abd El-Wahed, S.M. Al-Mousawi, S.G. Musharraf, et al., Marine natural products: a source of novel anticancer drugs, Mar. Drugs 17 (2019), https://doi.org/10.3390/md17090491.

[24] C. Alves, J. Silva, S. Pinteus, H. Gaspar, M.C. Alpoim, L.M. Botana, R. Pedrosa, From marine origin to therapeutics: the antitumor potential of marine algae-derived compounds, Front. Pharmacol. 9 (2018), https://doi.org/10.3389/fphar.2018.00777.

[25] A.R. Carroll, B.R. Copp, R.A. Davis, R.A. Keyzers, M.R. Prinsep, Marine natural products, Nat. Prod. Rep. 38 (2021) 362–413, https://doi.org/10.1039/D0NP00089B.

[26] R.D. Firn, C.G. Jones, The evolution of secondary metabolism - a unifying model, Mol. Microbiol. 37 (2000) 989–994, https://doi.org/10.1046/j.1365-2958.2000.02098.x.

[27] D. Giordano, D. Coppola, R. Russo, R. Denaro, L. Giuliano, F.M. Lauro, G. di Prisco, C. Verde, Marine microbial secondary metabolites: pathways, evolution and physiological roles, Adv. Microb. Physiol. 66 (2015) 357–428, https://doi.org/10.1016/bs.ampbs.2015.04.001.

[28] M. Conte, E. Fontana, A. Nebbioso, L. Altucci, Marine-derived secondary metabolites as promising epigenetic bio-compounds for anticancer therapy, Mar. Drugs 19 (2020), https://doi.org/10.3390/md19010015.

[29] L.A. Salvador-Reyes, H. Luesch, Biological targets and mechanisms of action of natural products from marine cyanobacteria, Nat. Prod. Rep. 32 (2015) 478–503, https://doi.org/10.1039/c4np00104d.

[30] G. Zinzalla, D.E. Thurston, Targeting protein-protein interactions for therapeutic intervention: a challenge for the future, Future Med. Chem. 1 (2009) 65–93, https://doi.org/10.4155/fmc.09.12.

[31] Guiry, M.D.G., G.M. AlgaeBase. World-wide electronic publication. Available online: ⟨https://www.algaebase.org⟩ (accessed on 18th June,2021).

[32] D. Rodrigues, C. Alves, A. Horta, S. Pinteus, J. Silva, G. Culioli, O.P. Thomas, R. Pedrosa, Antitumor and antimicrobial potential of bromoditerpenes isolated from the red alga, *Sphaerococcus coronopifolius*, Mar. Drugs 13 (2015) 713–726, https://doi.org/10.3390/md13020713.

[33] V. Smyrniotopoulos, A.C. de Andrade Tomaz, Md.F. Vanderlei de Souza, E. V. Leitão da Cunha, R. Kiss, V. Mathieu, E. Ioannou, V. Roussis, Halogenated diterpenes with *in vitro* antitumor activity from the red alga *Sphaerococcus coronopifolius*, Mar. Drugs 18 (2020) 29.

[34] W. Fenical, J. Finer, J. Clardy, Sphaerococcenol A; a new rearranged bromo-diterpene from the red alga *Sphaerococcus coronopifolius*. Tetrahedron Lett. 17 (1976) 731–734, https://doi.org/10.1016/S0040-4039(00)77936-6.

[35] S. Etahiri, V. Bultel-Poncé, C. Caux, M. Guyot, New bromoditerpenes from the red alga *Sphaerococcus coronopifolius*, J. Nat. Prod. 64 (2001) 1024–1027, https://doi.org/10.1021/np0002684.

[36] V. Smyrniotopoulos, C. Vagias, C. Bruyère, D. Lamoral-Theys, R. Kiss, V. Roussis, Structure and *in vitro* antitumor activity evaluation of brominated diterpenes from the red alga *Sphaerococcus coronopifolius*, Bioorg. Med. Chem. 18 (2010) 1321–1330, https://doi.org/10.1016/j.bmc.2009.12.025.

[37] T. Mosmann, Rapid colorimetric assay for cellular growth and survival: application to proliferation and cytotoxicity assays, J. Immunol. Methods 65 (1983) 55–63, https://doi.org/10.1016/0022-1759(83)90303-4.

[38] C. Alves, E. Serrano, J. Silva, C. Rodrigues, S. Pinteus, H. Gaspar, L.M. Botana, M. C. Alpoim, R. Pedrosa, *Sphaerococcus coronopifolius* bromoterpenes as potential cancer stem cell-targeting agents, Biomed. Pharmacother. 128 (2020), 110275, https://doi.org/10.1016/j.biopha.2020.110275.

[39] J. Silva, C. Alves, S. Pinteus, S. Mendes, R. Pedrosa, Neuroprotective effects of seaweeds against 6-hydroxidopamine-induced cell death on an in vitro human neuroblastoma model, BMC Complement. Altern. Med. 18 (2018) 58, https://doi.org/10.1186/s12906-018-2103-2.

[40] N.P. Singh, M.T. McCoy, R.R. Tice, E.L. Schneider, A simple technique for quantitation of low levels of DNA damage in individual cells, Exp. Cell Res. 175 (1988) 184–191, https://doi.org/10.1016/0014-4827(88)90265-0.

[41] C. Alves, J. Silva, S. Pinteus, E. Alonso, R. Alvariño, A. Duarte, D. Marmitt, M. I. Goettert, H. Gaspar, A. Alfonso, et al., Cytotoxic mechanism of sphaerodactylomelol, an uncommon bromoditerpene isolated from *Sphaerococcus coronopifolius*, Molecules 26 (2021) 1374.

[42] W. Harshbarger, C. Miller, C. Diedrich, J. Sacchettini, Crystal structure of the human 20S proteasome in complex with carfilzomib, Structure 23 (2015) 418–424, https://doi.org/10.1016/j.str.2014.11.017.

[43] G. Jones, P. Willett, R.C. Glen, A.R. Leach, R. Taylor, Development and validation of a genetic algorithm for flexible docking, J. Mol. Biol. 267 (1997) 727–748, https://doi.org/10.1006/jmbi.1996.0897.

[44] S. Salentin, S. Schreiber, V.J. Haupt, M.F. Adasme, M. Schroeder, PLIP: fully automated protein–ligand interaction profiler, Nucleic Acids Res. 43 (2015) W443–W447, https://doi.org/10.1093/nar/gkv315.

[45] R. Gavioli, S. Vertuani, M.G. Masucci, Proteasome inhibitors reconstitute the presentation of cytotoxic T-cell epitopes in Epstein-Barr virus–associated tumors, Int. J. Cancer 101 (2002) 532–538, https://doi.org/10.1002/ijc.10653.

[46] D.M. Pereira, S.E. Gomes, P.M. Borralho, C.M.P. Rodrigues, MEK5/ERK5 activation regulates colon cancer stem-like cell properties, Cell Death Discov. 5 (2019) 68, https://doi.org/10.1038/s41420-019-0150-1.

[47] C. Yokoyama, Y. Sueyoshi, M. Ema, Y. Mori, K. Takaishi, H. Hisatomi, Induction of oxidative stress by anticancer drugs in the presence and absence of cells, Oncol. Lett. 14 (2017) 6066–6070, https://doi.org/10.3892/ol.2017.6931.

[48] I.R. Indran, G. Tufo, S. Pervaiz, C. Brenner, Recent advances in apoptosis, mitochondria and drug resistance in cancer cells, Biochim. Et. Biophys. Acta (BBA) - Bioenerg. 1807 (2011) 735–745, https://doi.org/10.1016/j.bbabio.2011.03.010.

[49] R. Corvi, F. Madia, In vitro genotoxicity testing-Can the performance be enhanced? Food Chem. Toxicol. 106 (2017) 600–608, https://doi.org/10.1016/j.fct.2016.08.024.

[50] J.B. Almond, G.M. Cohen, The proteasome: a novel target for cancer chemotherapy, Leukemia 16 (2002) 433 (+).

[51] A. Zeuner, M. Todaro, G. Stassi, R. De Maria, Colorectal cancer stem cells: from the crypt to the clinic, Cell Stem Cell 15 (2014) 692–705, https://doi.org/10.1016/j.stem.2014.11.012.

[52] D.J. Newman, G.M. Cragg, Natural products as sources of new drugs over the nearly four decades from 01/1981 to 09/2019, J. Nat. Prod. 83 (2020) 770–803, https://doi.org/10.1021/acs.jnatprod.9b01285.

[53] A. Singh, B.S. Kumar, H. Iqbal, S. Alam, P. Yadav, A.K. Verma, F. khan, K. Shanker, K. Hanif, A.S. Negi, et al., Antihypertensive activity of diethyl-4,4′-dihydroxy-8,3′-neolign-7,7′-dien-9,9′-dionate: a continuation study in L-NAME treated wistar rats, Eur. J. Pharmacol. 858 (2019), 172482, https://doi.org/10.1016/j.ejphar.2019.172482.

[54] A. Srivastava, K. Fatima, E. Fatima, A. Singh, A. Singh, A. Shukla, S. Luqman, K. Shanker, D. Chanda, F. Khan, et al., Fluorinated benzylidene indanone exhibits antiproliferative activity through modulation of microtubule dynamics and antiangiogenic activity, Eur. J. Pharm. Sci. 154 (2020), 105513, https://doi.org/10.1016/j.ejps.2020.105513.

[55] M. Huang, J.J. Lu, J. Ding, Natural products in cancer therapy: past, present and future, Nat. Prod. Bioprospecting 11 (2021) 5–13, https://doi.org/10.1007/s13659-020-00293-7.

[56] V. Smyrniotopoulos, A. Quesada, C. Vagias, D. Moreau, C. Roussakis, V. Roussis, Cytotoxic bromoditerpenes from the red alga *Sphaerococcus coronopifolius*, Tetrahedron 64 (2008) 5184–5190, https://doi.org/10.1016/j.tet.2008.03.042.

[57] Y. Ling, J. Liu, J. Qian, C. Meng, J. Guo, W. Gao, B. Xiong, C. Ling, Y. Zhang, Recent advances in multi-target drugs targeting protein kinases and histone deacetylases in cancer therapy, Curr. Med. Chem. 27 (2020) 7264–7288, https://doi.org/10.2174/0929867327666200102115720.

[58] B. Pucci, M. Kasten, A. Giordano, Cell cycle and apoptosis, Neoplasia 2 (2000) 291–299, https://doi.org/10.1038/sj.neo.7900101.

[59] F.Q. Alenzi, Links between apoptosis, proliferation and the cell cycle, Br. J. Biomed. Sci. 61 (2004) 99–102.

[60] S. Maddika, S.R. Ande, S. Panigrahi, T. Paranjothy, K. Weglarczyk, A. Zuse, M. Eshraghi, K.D. Manda, E. Wiechec, M. Los, Cell survival, cell death and cell cycle pathways are interconnected: implications for cancer therapy, Drug Resist. Updates 10 (2007) 13–29, https://doi.org/10.1016/j.drup.2007.01.003.

[61] O. Rixe, T. Fojo, Is cell death a critical end point for anticancer therapies or is cytostasis sufficient? Clin. Cancer Res. 13 (2007) 7280–7287, https://doi.org/10.1158/1078-0432.ccr-07-2141.

[62] M. Redza-Dutordoir, D.A. Averill-Bates, Activation of apoptosis signalling pathways by reactive oxygen species, Biochim. Et. Biophys. Acta (BBA) - Mol. Cell Res. 1863 (2016) 2977–2992, https://doi.org/10.1016/j.bbamcr.2016.09.012.

[63] M. Singh, H. Sharma, N. Singh, Hydrogen peroxide induces apoptosis in HeLa cells through mitochondrial pathway, Mitochondrion 7 (2007) 367–373, https://doi.org/10.1016/j.mito.2007.07.003.

[64] S. Pinteus, M. Lemos, J. Silva, C. Alves, A. Neugebauer, R. Freitas, A. Duarte, R. Pedrosa, An Insight into *Sargassum muticum* cytoprotective mechanisms against oxidative stress on a human cell in vitro model, Mar. Drugs 15 (2017) 353.

[65] C.-I. Yu, C.-Y. Chen, W. Liu, P.-C. Chang, C.-W. Huang, K.-F. Han, I.-P. Lin, M.-Y. Lin, C.-H. Lee, Sandensolide induces oxidative stress-mediated apoptosis in oral cancer cells and in zebrafish xenograft model, Mar. Drugs 16 (2018) 387.

[66] W.-T. Chang, Y.-D. Bow, P.-J. Fu, C.-Y. Li, C.-Y. Wu, Y.-H. Chang, Y.-N. Teng, R.-N. Li, M.-C. Lu, Y.-C. Liu, et al., A marine terpenoid, heteronemin, induces both the apoptosis and ferroptosis of hepatocellular carcinoma cells and involves the ROS and MAPK pathways, Oxid. Med. Cell. Longev. 2021 (2021), 7689045, https://doi.org/10.1155/2021/7689045.

[67] L.R. Velatooru, C.B. Baggu, V.R. Janapala, Spatane diterpinoid from the brown algae, *Stoechospermum marginatum* induces apoptosis via ROS induced mitochondrial mediated caspase dependent pathway in murine B16F10 melanoma cells, Mol. Carcinog. 55 (2016) 2222–2235, https://doi.org/10.1002/mc.22463.

[68] M. Koul, A. Kumar, R. Deshidi, V. Sharma, R.D. Singh, J. Singh, P.R. Sharma, B. A. Shah, S. Jaglan, S. Singh, Cladosporol A triggers apoptosis sensitivity by ROS-mediated autophagic flux in human breast cancer cells, BMC Cell Biol. 18 (2017) 26, https://doi.org/10.1186/s12860-017-0141-0.

[69] J. Li, B. Xu, J. Cui, Z. Deng, N.J. de Voogd, P. Proksch, W. Lin, A.–I. Globostelletins, cytotoxic isomalabaricane derivatives from the marine sponge *Rhabdastrella globostellata*, Bioorg. Med. Chem. 18 (2010) 4639–4647, https://doi.org/10.1016/j.bmc.2010.05.029.

[70] A. Noda, E. Sakai, H. Kato, F. Losung, R.E. Mangindaan, N.J. de Voogd, H. Yokosawa, S. Tsukamoto, Strongylophorines, meroditerpenoids from the marine sponge *Petrosia corticata*, function as proteasome inhibitors, Bioorg. Med. Chem. Lett. 25 (2015) 2650–2653, https://doi.org/10.1016/j.bmcl.2015.04.075.

[71] J. Cotas, V. Marques, M.B. Afonso, C.M.P. Rodrigues, L. Pereira, Antitumour potential of *Gigartina pistillata* carrageenans against colorectal cancer stem cell-enriched tumourspheres, Mar. Drugs 18 (2020) 50, https://doi.org/10.3390/md18010050.

[72] Y.T. Ahn, M.S. Kim, Y.S. Kim, W.G. An, Astaxanthin reduces stemness markers in BT20 and T47D breast cancer stem cells by inhibiting expression of pontin and mutant p53, Mar. Drugs 18 (2020) 577.

[73] E.A. Guzmán, T.P. Pitts, P.L. Winder, A.E. Wright, The marine natural product furospinulosin 1 induces apoptosis in MDA-MB-231 triple negative breast cancer cell spheroids, but not in cells grown traditionally with longer treatment, Mar. Drugs 19 (2021), https://doi.org/10.3390/md19050249.

[74] B.-Y. Hu, S.-X. Wang, Y.-M. Yan, J.-W. Liu, D.-P. Qin, Y.-X. Cheng, Spiromyrrhenes A–D: unprecedented diterpene–sesquiterpene heterodimers as intermolecular [4 + 2] cycloaddition products from *Resina Commiphora* that inhibit tumor stemness in esophageal cancer, Org. Chem. Front. 7 (2020) 2710–2718, https://doi.org/10.1039/D0QO00656D.

[75] W.-J. Yuan, X. Ding, Z. Wang, B.-J. Yang, X.-N. Li, Y. Zhang, D.-Z. Chen, S.-L. Li, Q. Chen, Y.-T. Di, et al., Two novel diterpenoid heterodimers, Bisebracteolasins A and B, from *Euphorbia ebracteolata* Hayata, and the cancer chemotherapeutic potential of Bisebracteolasin A, Sci. Rep. 7 (2017) 14507, https://doi.org/10.1038/s41598-017-14637-w.

[76] Y. Iida, M. Okamoto-Katsuyama, S. Maruoka, K. Mizumura, T. Shimizu, S. Shikano, M. Hikichi, M. Takahashi, K. Tsuya, S. Okamoto, et al., Effective ferroptotic small-cell lung cancer cell death from SLC7A11 inhibition by sulforaphane, Oncol. Lett. 21 (2021) 71, https://doi.org/10.3892/ol.2020.12332.

[77] W.R. Taylor, S.R. Fedorka, I. Gad, R. Shah, H.D. Alqahtani, R. Koranne, N. Kuganesan, S. Dlamini, T. Rogers, A. Al-Hamashi, et al., Small-molecule ferroptotic agents with potential to selectively target cancer stem cells, Sci. Rep. 9 (2019) 5926, https://doi.org/10.1038/s41598-019-42251-5.